Tetrahedron 70 (2014) 3909–3914

Contents lists available at ScienceDirect

Tetrahedron

journal homepage: www.elsevier.com/locate/tet

From *N*,*N*-diphenyl-*N*-naphtho[2,1-*b*]thieno[2,3-*b*:3′,2′-*d*]dithiophene-5-yl-amine to propeller-shaped *N*,*N*,*N*-tri(naphtho[2,1-*b*]thieno[2,3-*b*:3′,2′-*d*]dithiophene-5-yl)-amine: syntheses and structures

Chunli Li [a,*,†], Yongqing Zhang [a,†], Sheng Zhang [a], Jianwu Shi [a], Yuhe Kan [b], Hua Wang [a,*]

[a] *Key Lab for Special Functional Materials of Ministry of Education, Henan University, Kaifeng 475004, China*
[b] *Jiangsu Province Key Laboratory for Chemistry of Low Dimensional Materials, School of Chemistry and Chemical Engineering, Huaiyin Normal University, Huaian 223300, China*

ARTICLE INFO

Article history:
Received 23 November 2013
Received in revised form 26 February 2014
Accepted 10 April 2014
Available online 18 April 2014

Keywords:
Helicenyl amines
Synthesis
Crystal structures

ABSTRACT

Three unique propeller-shaped helicenyl amines compounds: *N*,*N*-diphenyl-*N*-naphtho[2,1-*b*]thieno[2,3-*b*:3′,2′-*d*]dithiophene-5-yl-amine (**1**), *N*-phenyl-*N*,*N*-di(naphtho[2,1-*b*]thieno[2,3-*b*:3′,2′-*d*]dithiophene-5-yl)amine (**2**), and *N*,*N*,*N*-tri(naphtho[2,1-*b*]thieno[2,3-*b*:3′,2′-*d*]dithiophene-5-yl)amine (**3**) were efficiently synthesized by Wittig reaction and oxidative photocyclization. The crystal structures of **1**, **2** and molecular configuration optimization (DFT-B3LYP/6-31+G(d)) of **3** reveal that the steric hindrance from the moiety of trithia[5]helicene effectively forces the nitrogen atom and the three bonded carbon atoms to coplanar and the interplanar angles of the facing terminal thiophene ring and benzene ring becoming larger when the helical arm increased from **1** to **3**. Electrochemical properties and UV–vis absorption behaviors of **1**, **2**, **3** were primarily determined by the moiety of trithia[5]helicene.

1. Introduction

Helicenes are polycyclic aromatic compounds with unique helical structure and inherent chirality formed by *ortho*-fused benzene or other aromatic rings. Due to their structurally unique helical chirality, helicenes and helicene-like compounds have attracted great attention as a source of chirality in asymmetric synthesis,[1] chiral material,[1b,2] circularly polarized luminescence material,[1b,3] and chiral discriminator of biomolecules.[2c,3d]

Generally, the helically shaped organic fused molecules are of two types: carbohelicenes and heterohelicenes.[1a,4] Compared with carbohelicenes, heterohelicenes have a nicely delocalized π-electron system with a high thermal stability, which allows them to exhibit interesting opto- and photo-electronic properties.[5] Thiahelicenes, as a kind of typical heterohelicenes, have been intensively studied due to their prospective applications in fields, such as light-emitting devices and chemosensors.[6,7] However, structure types of thiahelicene-based compounds reported are very limited until now.[1a] Our research group has studied the preparation of thiahelicenes and double thiahelicenes for years.[8] As part of our continuing interest, we try to design and synthesize novel helicene-based compounds, in which helicene is employed as a moiety. As we all know, steric hindrance between the phenyl rings grafted on the central nitrogen atom of triphenylamine (TPA) generates the typical propeller shape of the molecule.[9] In this paper, TPA is employed for the exploitation of unique structure helicene-based compounds, three [5]helicene-based novel propeller-shaped aryl amines were synthesized through Witting and oxidative photocyclization reactions, started from TPA and dithieno[2,3-*b*:3′,2′-*d*]thiophene-2-carbaldehyde (**4**). In addition, the crystal structures of **1**, **2** and molecular configuration optimization (DFT-B3LYP/6-31+G(d)) of **3** were studied for description of such novel compounds.

2. Results and discussion

2.1. The synthesis of 1, 2, and 3

Dithieno[2,3-*b*:3′,2′-*d*]thiophene-2-carbaldehyde (**4**) was prepared via multi-step moisture sensitive reactions with 3-bromothiophene as substrate according to the method reported by our early research.[10] Witting salts of [4-(*N*,*N*-diphenylamino)benzyl]triphenylphosphonium bromide (TPA-$PPh_3 \cdot Br$), [4,4′-(*N*-phenylamino)dibenzyl] di(triphenyl-phosphonium)dibromide

---

[*] Corresponding authors. Tel.: +86 371 23897112 (o); fax: +86 371 23881358; e-mail addresses: chunli79@126.com (C. Li), hwang@henu.edu.cn (H. Wang).

[†] These authors contributed equally to this work.

0040-4020/$ – see front matter © 2014 Elsevier Ltd. All rights reserved.
http://dx.doi.org/10.1016/j.tet.2014.04.031

($TPA-(PPh_3 \cdot Br)_2$), and [4,4′,4″-(amino)tribenzyl]-tri(-triphenylphosphonium) tribromide ($TPA-(PPh_3 \cdot Br)_3$) were synthesized according to the literature[11] via steps of formylation, sodium borohydride ($NaBH_4$) reduction, and bromination started from TPA (Scheme 1).

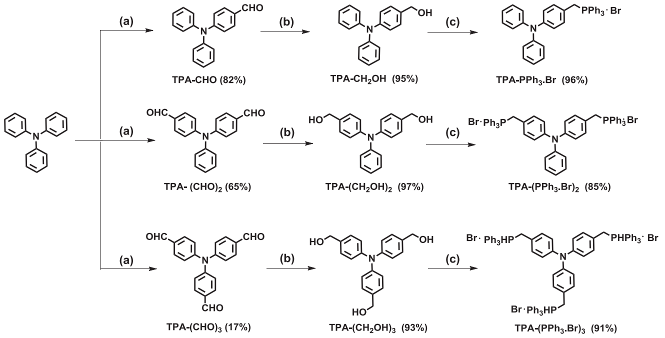

Scheme 1. Synthetic route to $TPA-PPh_3 \cdot Br$, $TPA-(PPh_3 \cdot Br)_2$, $TPA-(PPh_3 \cdot Br)_3$. (a) $POCl_3$, 80–90 °C/48 h, DMF (b) $NaBH_4$, CH_2Cl_2, rt, 2 h, EtOH (c) $PPh_3 \cdot HBr$, reflux, 2 h, $CHCl_3$.

The synthetic route of **1**, **2**, and **3** is outlined in Scheme 2. Wittig reaction between $TPA-PPh_3 \cdot Br$ and **4** was employed in the presence of potassium *tert*-butoxide (*t*-BuOK) in tetrahydrofuran (THF) for making 4-(2-(dithieno[2,3-*b*:3′,2′-*d*]-thiophene)-2-yl)vinylphenyl-*N*,*N*-diphenylamine (**5**), which gives a mixture of (*Z*)-**5** and (*E*)-**5**. Then the dry mixture of (*Z*)-**5** and (*E*)-**5** was dissolved in THF to reflux in the presence of catalytic amount iodine, pure (*E*)-**5** was obtained in yield of 51%.[11] The formation of (*E*)-**5** involved one new carbon–carbon double bond formation. Under the same conditions, bis[(*E*)-4-(2-(dithieno[2,3-*b*:3′,2′-*d*]thiophene)-2-yl)vinylphenyl]-*N*-phenylamine ((*E*)-**6**) was obtained with yield of 46%. The formation of (*E*)-**6** involved two new carbon–carbon double bonds formation. Tris[(*E*)-4-(2-dithieno[2,3-*b*:3′,2′-*d*]thiophen-2-yl-vinyl)phenyl]amine ((*E*)-**7**) was efficiently synthesized in a yield of 68% via Wittig reaction. The synthesis of (*E*)-**7** requires the formation of three new carbon–carbon double bonds, thus Wittig reaction is very efficient and only single (*E*)-typed configuration formed from ^1H NMR analysis.

Helicenyl amine compound **1** was obtained through oxidative photocyclization reaction in the presence of iodine in dry benzene via irradiation with a 450 W unfiltered Hg medium pressure lamp of (*E*)-**5** with a yield of 38%. Compounds **2** and **3** were also efficiently synthesized in yield of 65% and 34%, respectively, under the same conditions as those in making **1** via oxidative photocyclization reactions from (*E*)-**6** and (*E*)-**7**, in which two and three the moieties of trithia[5]helicene were formed. Without solubilizing groups, compounds **1**, **2**, and **3** are very insoluble. It is tough to work up and hard to obtain their ^{13}C NMR spectra.

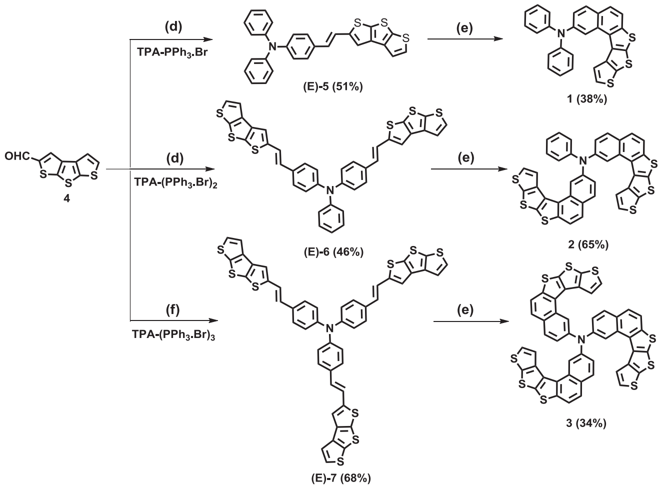

Scheme 2. Synthetic route of **1**, **2**, and **3**. (d) (i) *t*-BuOK, rt, 6 h, THF (ii) I_2, reflux, 6 h, THF (e) I_2, *hν*/benzene (f) *t*-BuOK, rt, 6 h, THF.

2.2. Crystal structures of 1, 2, (*E*)-5 and theoretical calculations of 3

The molecular structures of compounds **1**, **2**, (*E*)-**5** are all confirmed by single-crystal X-ray analysis (Fig. 1). Compound (*E*)-**5** crystallizes into the monoclinic, space group *Pc*, and shows the *E* stereoisomer. The values of the bond angles C-N-C are 117.3°(C1-N1-C7), 120.0°(C1-N1-C13), and 121.0°(C7-N1-C13), respectively. The mean value of N-C bond lengths is 1.441 Å, which are longer than that in triphenylamine (1.419 Å).[12] The nitrogen atom deviates from the plane of the bonded C atoms by 0.109 Å (mean value), which is larger than that in triphenylamine (0.08 Å).[12] In (*E*)-**5**, dithieno[2,3-*b*:3′,2′-*d*]thiophene is approximately coplanar with torsion of 7.19° (C22-C23-C25-C27). Multiple short interactions including S···S (3.439, 3.561, 3.519 Å) and C···S (3.494, 3.335 Å) interactions could be observed from its crystal packing.

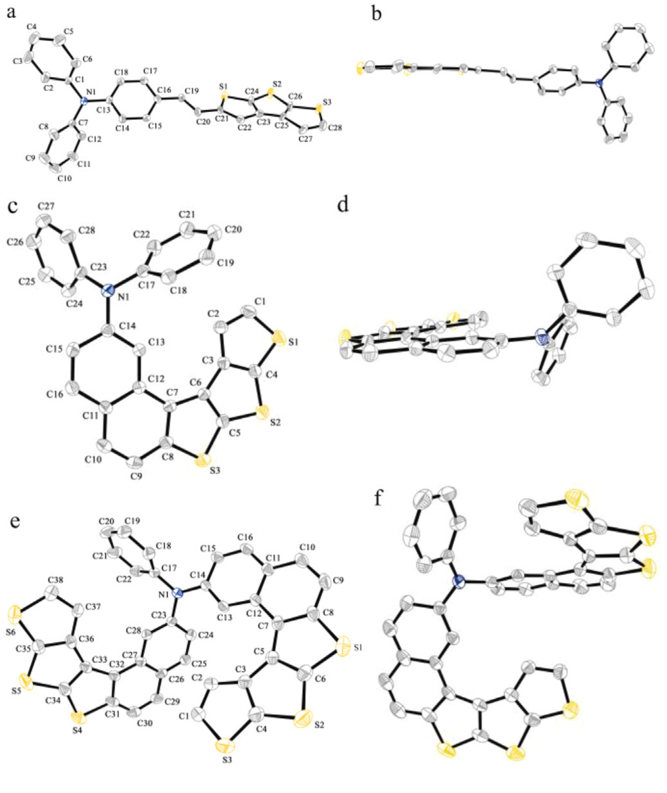

Fig. 1. Molecular structure and conformation for (*E*)-**5**, **1**, and **2**. (a) Top view for (*E*)-**5**, (b) side view for (*E*)-**5**, (c) top view for **1**, (d) side view for **1**, (e) top view for **2**, (f) side view for **2**. Carbon, nitrogen, and sulfur atoms are depicted with thermal ellipsoids set at the 30% probability level. The hydrogen atoms are omitted for clarity.

The crystal structures of **1**, **2** and molecular configuration optimization (DFT-B3LYP/6-31+G(d)) of **3** reveal that the formation of the moieties of trithia[5]helicene significantly influences their structural parameters: (1) **1** belongs to monoclinic, space group *P*2(1)/*c*, **2** crystallizes in the orthorhombic, space group *Pna*2(1). Bond lengths of C-N and bond angles of C-N-C were listed in Table 1. From the data in Table 1, we can see that bond angles of C-N-C and

Table 1
Bond lengths (Å), bond angles (°), distortion angles (defined by the sum of the three dihedral angles) (°), and interplanar angles of the facing terminal thiophene ring and benzene ring of **1**, **2**, **3**

	1	**2**	**3**
Bond lengths			
C14–N1	1.426	1.409	
C17–N1	1.439	1.420	
C23–N1	1.425	1.417	
C2–N1			1.422
C3–N1			1.419
C4–N1			1.421
Bond angles			
C23–N1–C17	117.9	119.6	
C14–N1–C17	119.1	119.2	
C14–N1–C23	118.2	119.9	
C2–N1–C4			119.3
C2–N1–C3			120.2
C3–N1–C4			119.9
Distortion angles			
	7.7 (C2–C3–C6–C7–C12–C13)	10.0 (C28–C27–C32–C33–C36–C37) 9.5 (C13–C12–C7–C5–C3–C2)	22.6 (C14–C13–C23–C34–C37–C40) 22.7 (C9–C8–C27–C43–C46–C49) 18.5 (C19–C18–C31–C52–C55–C58)
Interplanar angles			
	5.8 (C2–C3–C6–C7–C12–C13)	7.7 (C28–C27–C32–C33–C36–C37) 7.8 (C13–C12–C7–C5–C3–C2)	17.3 (C14–C13–C23–C34–C37–C40) 17.5 (C9–C8–C27–C43–C46–C49) 14.7 (C19–C18–C31–C52–C55–C58)

bond lengths of C-N tend to be more averaged, and bond angles of C-N-C are all close to 120°; (2) With the formation of moieties of trithia[5]helicene, helical structures are compressed (Figs. 1, 2, Table 1); (3) The steric hindrance from the moieties of trithia[5] helicene effectively forces nitrogen atom and the three bonded carbon atoms to coplanar, which the central nitrogen deviates from the plane of the bonded carbon atoms in **1**, **2**, and **3** by 0.183, 0.097, 0.062 Å, respectively; (4) The steric hindrance from the moieties of trithia[5]helicene compels the distortions (defined by the sum of the three dihedral angles) and interplanar angles of the facing terminal thiophene ring and benzene ring becoming larger (Table 1). The bond angles of C-N-C in the molecules of **1**, **2**, and **3** are all close to 120°, which corresponds to the sp^2 hybridization of the nitrogen bonding orbitals. Therefore, this shows that the lone electron pair (l.e.p.) of the nitrogen atom in **1**, **2**, and **3** occupies the p orbital, which favors the realization of the intramolecular p–π interaction.[12]

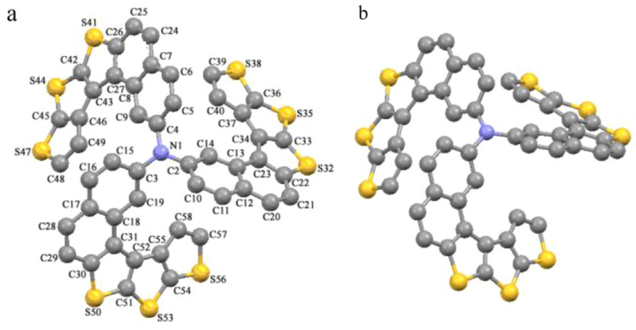

Fig. 2. Optimized molecular structure and conformation for **3**. (a) Top view for **3**, (b) side view for **3**.

Racemate of (R,R)-**2**/(S,S)-**2** appeared in a 1:1 ratio, and no (R,S)-**2** or (S,R)-**2** was observed in the packing of **2**. Therefore, the diastereoselectivity of oxidative photocyclization for the synthesis of **2** is high. There are multiple short interactions in the crystal packings of **1** (S⋯S, 3.474, 3.357 Å) and **2** (S⋯S 3.553 Å, S⋯C 3.478, 3.490, 3.405 Å, C⋯C, 3.321, 3.386 Å).

2.3. UV–vis properties

UV–vis absorption spectra of (E)-**5**, (E)-**6**, (E)-**7**, **1**, **2**, and **3** in chloroform are shown in Fig. 3. Compounds (E)-**5**, (E)-**6**, (E)-**7** exhibit two major absorbance bands in the range of 297–305 nm and 390–414 nm. The first absorption band at around 297–305 nm contributes to the triphenylamine.[9b] The second absorption band at around 390–314 nm contributes to (E)-4-(2-(dithieno[2,3-b:3′,2′-d]thiophene)-2-yl)vinylphenyl. With the increasing of (E)-4-(2-(dithieno[2,3-b:3′,2′-d]thiophene)-2-yl)vinylphenyl, small bathochromic shifts ((E)-**5**, λ_{max}=390 nm; (E)-**6**, λ_{max}=412 nm; (E)-**7**, λ_{max}=414 nm) and approximately linear increase of the integrated absorbance are observed. The formation of trithia[5]helicene causes significant blue shifts and decreasing of the integrated absorbance from (E)-**5**, (E)-**6**, (E)-**7** to corresponding **1**, **2**, and **3**. Compounds **1**, **2**, and **3** show two major absorbance bands at l_{max}≈271–292 nm and λ_{max}≈378–382 nm. Increasing of the moiety of trithia[5]helicene does not induce apparently absorbance bands shift (**1**, λ_{max}=377 nm; **2**, λ_{max}=380 nm; **3**, λ_{max}=377 nm), but the extinction coefficient increased, significantly. On the basis of the absorption onsets at 403–414 nm, E_g≈3.0 eV is estimated for

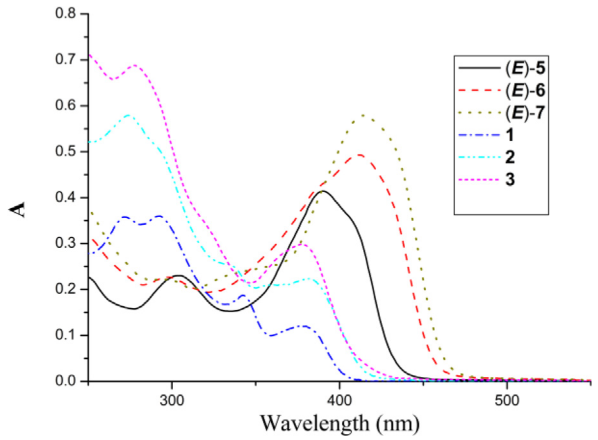

Fig. 3. UV–vis spectra for (E)-**5**, (E)-**6**, (E)-**7**, **1**, **2**, and **3** in chloroform at room temperature ([C]=1×10^{-5} M).

1 (E_g=3.1 eV), **2** (E_g=3.0 eV), and **3** (E_g=3.0 eV). The results demonstrated that the absorption behavior and E_g of **1**, **2**, **3** mainly affected by the moiety of trithia[5]helicene.

2.4. Electrochemical behaviors

The cyclic voltammetry behaviors of (*E*)-**5**, (*E*)-**6**, (*E*)-**7**, **1**, **2**, and **3** were investigated to determine their electrochemical properties (Fig. 4). All the compounds show two quasi-reversible oxidation peaks. The onset value of the first oxidative peak (E^1_{onset}) is 0.46 V for **1**, 0.46 V for **2**, 0.41 V for **3**, 0.33 V for (*E*)-**5**, 0.23 V for (*E*)-**6**, and 0.26 V for (*E*)-**7**, respectively. The onset value of the second oxidative peak (E^2_{onset}) is 0.95 V for **1**, 0.88 V for **2**, 0.88 V for **3**, 0.60 V for (*E*)-**5**, 0.51 V for (*E*)-**6**, 0.54 V for (*E*)-**7**, respectively. It is clear that the onset values of **1**, **2**, and **3** are higher than that of (*E*)-**5**, (*E*)-**6**, and (*E*)-**7** both for the first and second oxidative peak. This indicates that **1**, **2**, and **3** are more difficult to loss electrons than their precursors. Moreover, the onset values of the first oxidation peaks are almost same in **1**, **2**, and **3**, which implies that the HOMO levels of **1**, **2**, and **3** are nearly equal.

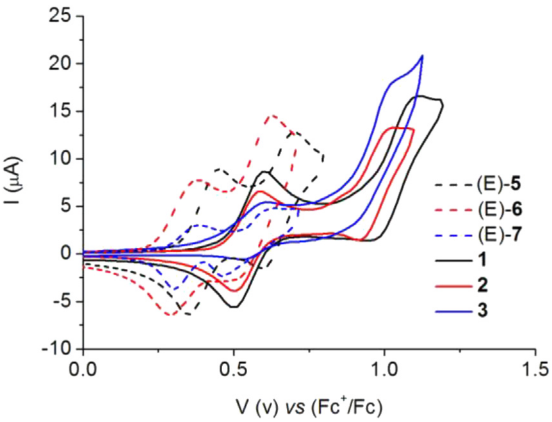

Fig. 4. Cyclic voltammograms of **1**, **2**, **3**, (*E*)-**5**, (*E*)-**6**, and (*E*)-**7** ([C]=1×10^{-3} M) in CH_2Cl_2 containing 0.1 M TBAHFP at 100 mV s^{-1}.

3. Conclusion

In conclusion, with TPA and **4** as starting materials, three unique propeller-shaped helicenyl amines **1**, **2**, and **3** were efficiently constructed via Wittig and oxidative photocyclization reactions in total yield of 19%, 30%, and 23%, respectively. The increasing of helical arm from 1 to 3 significantly influences the structural parameters of **1**, **2**, and **3**. (1) Bond angles of C-N-C and bond lengths of C-N tend to be more averaged; (2) The steric hindrance from helical arm trithia[5]helicene effectively forces the nitrogen atom and the three bonded carbon atoms to coplanar; (3) The interplanar angles of the facing terminal thiophene ring and benzene ring becomes larger. The lone electron pair (l.e.p.) of the nitrogen atom in **1**, **2**, and **3** occupies the p orbital, which favors the realization of the intramolecular p–π interaction. Cyclic voltammetry and UV–vis absorption behaviors study of **1**, **2**, **3** show that UV–vis absorption behaviors, optical band gap, and HOMO levels of **1**, **2**, **3** were primarily determined by the moiety of trithia[5]helicene. This work gives an interesting example in the exploitation for unique helicene compounds.

4. Experimental section

4.1. Materials and general methods

Ether and tetrahydrofuran (THF) for use were freshly distilled from sodium/benzophenone prior to use. Concentration of *n*-BuLi (hexane) was determined by titration with *N*-pivaloyl-*o*-toluidine. Column chromatography was carried out on silica gel (300–400 mesh). Analytical thin-layer chromatography was performed on glass plates of Silica Gel GF-254 with detection by UV. Standard techniques for synthesis under inert atmosphere, using gasbag and Schlenk glassware equipped with an 8-mm PTFE vacuum stop-cock, were employed. All starting materials and reagents were commercially available.

^{1}H and ^{13}C NMR spectra were recorded on a Bruker AVANCE400M spectrometer. NMR spectra were obtained using chloroform-*d* ($CDCl_3$) and pyridine-d_5 as solvent. The chemical shift references were as follows: (^{1}H) $CDCl_3$, 7.26 ppm ($CHCl_3$); (^{13}C) $CDCl_3$, 77.00 ppm ($CDCl_3$); (^{13}C) pyridine-d_5, 150.35 ppm, 135.91 ppm, 123.87 ppm (pyridine-d_5). IR spectra were obtained using an FT-IR instrument, equipped with an ATR sampling accessory. HRMS spectra were carried out at Micromass GCT (TOF MS EI$^+$) or IonSpec 4.7 T FTMS (MALDI). Melting point determination was taken on a Melt-Temp apparatus and was uncorrected. UV–vis spectra were obtained with a double-beam spectrophotometer at room temperature.

The X-ray crystallographic analyses were performed using crystals of **5** with the size 0.45×0.36×0.23 mm, **1** with the size 0.22×0.18×0.14 mm, and **2** with the size 0.60×0.57×0.12 mm. The intensity data were collected with the ω scan mode (293(2) K) on a diffractometer with CCD detector using Mo Kα radiation (λ=0.71073 Å). The data were corrected for Lorentz and polarization effects and absorption corrections were performed using SADABS program. The crystal structures were solved using the SHELXTL program and refined using full matrix least squares. The positions of hydrogen atoms were calculated theoretically and included in the final cycles of refinement in a riding model along with attached carbons. Further details are in the deposited CIFs. Single crystals of (*E*)-**5**, **1**, and **2** suitable for X-ray analysis were obtained by slow evaporation from $CHCl_3$, THF, and $CHCl_3/CH_3OH$, respectively.

Cyclic voltammetry (CV) was performed on a CHI660a electrochemical analyzer with a three-electrode cell in a solution of 0.1 M tetrabutylammonium hexafluorophosphate (Bu_4NPF_6) dissolved in CH_2Cl_2. A platinum electrode (0.6 cm^2), a Pt wire, and an Ag/AgCl electrode were used as the working electrode, counter electrode, and reference electrode, respectively. Its potential was calibrated by the ferrocene/ferrocenium (0.65 V vs Ag/AgCl in CH_2Cl_2).

Molecular configuration optimization was carried out at DFT-B3LYP/6-31+G(d) level. For each stationary point, harmonic frequencies were computed at the fully optimized geometries, which allowed the assignment of the structures as minima. All these calculations were performed with Gaussian 03[13] program in Intel Core i7 computer.

4.2. Synthesis and characterization

*4.2.1. Synthesis of (E)-4-(2-(dithieno[2,3-b:3′,2′-d]thiophene)-2-yl) vinylphenyl-N,N-diphenylamine ((E)-**5**).* Dithieno[2,3-*b*:3′,2′-*d*] thiophene-2-carbaldehyde (**4**) (0.30 g, 1.34 mmol) and TPA-$PPh_3\cdot$Br (0.88 g, 1.47 mmol, 1.1 equiv) were dissolved in anhydrous tetrahydrofuran (15 mL), solution of potassium *tert*-butoxide (0.38 g, 3.34 mmol, 2.5 equiv) in anhydrous tetrahydrofuran (10 mL) were added dropwise at 0 °C, and then the reaction mixture was warmed slowly up to ambient temperature stir for 6 h. The reaction mixture was quenched with H_2O (10 mL) and extracted with $CHCl_3$ (3×5 mL), then washed with saturated $NaHCO_3$ (2×20 mL) and H_2O (20 mL). The organic layer was dried over anhydrous $MgSO_4$. After the solvent was removed under vacuum, the dry solid was dissolved in 20 mL THF to reflux in the presence of catalysis amount iodine for 6 h. The reaction mixture was added to diluted solution sodium hydroxide in order to remove iodine, then extracted with $CHCl_3$ (3 × 10 mL). Organic layer was dried with anhydrous sodium sulfate and removed the solvent, and was purified by column chromatography on silica gel with petrol ether, and then petrol ether/$CHCl_3$ (3:1, v/v) as eluent to give (*E*)-**5** (0.32 g, 51%) as a yellow solid. Mp: 187–188 °C. ^{1}H NMR ($CDCl_3$, 400 MHz) δ (ppm) 7.39 (d, J=5.2 Hz, 1H), 7.37–7.33 (m, 3H), 7.30–7.25 (m, 5H), 7.17–7.10 (m, 5H), 7.07–7.02 (m, 4H), 6.86 (d, J=16 Hz, 1H), ^{13}C NMR ($CDCl_3$, 100 MHz): δ 147.4, 145.9, 138.54, 138.48, 138.3, 137.2, 130.6, 129.3, 127.7, 127.1, 124.5, 123.4, 123.1, 120.6, 118.8, 117.1. IR (KBr): 2919, 1590, 1384, 1331, 1274, 1175, 696 cm^{-1}. HRMS (Tesla FTMS): found 465.0674, $C_{28}H_{19}NS_3$ requires 465.0661.

*4.2.2. Synthesis of N,N-diphenyl-N-naphtho[2,1-b]thieno[2,3-b:3′,2′-d]dithiophene-5-yl-amine (**1**).* To a solution of (*E*)-**5** (50.0 mg, 0.11 mmol) in dry benzene (50 mL), iodine (13.7 mg, 0.05 mmol, 0.5 equiv) was added. The reaction solution was irradiated with a 450 W unfiltered Hg medium pressure lamp. The reaction was monitored by TLC every 20 min, and irradiation was stopped when the (*E*)-**5** was consumed up. After normal workup, the crude product was purified by column chromatography on silica gel with petrol ether (60–90 °C)/$CHCl_3$ (7:1, v/v) as eluent. The collected product was dissolved in $CHCl_3$ and precipitated with MeOH. The precipitate was collected by filtration to afford pale yellow solid **1** (20 mg, 38%). Mp: 173–174 °C. ^{1}H NMR (400 MHz, $CDCl_3$): δ 8.56 (d, J=2.0 Hz, 1H), 7.86 (d, J=8.8 Hz, 1H), 7.73 (d, J=8.8 Hz, 1H), 7.69 (d, J=8.8 Hz, 1H), 7.45 (dd, J=8.8, 2.4 Hz, 1H), 7.36 (t, J=7.8 Hz, 4H), 7.28–7.25 (m, 4H), 7.15 (t, J=7.4 Hz, 2H), 7.04 (d, J=5.6 Hz, 1H), 6.63 (d, J=5.6 Hz, 1H), ^{13}C NMR ($CDCl_3$, 100 MHz): δ 148.1, 146.6, 141.2, 139.8, 139.3, 138.7, 133.9, 130.1, 129.7, 129.5, 128.3, 127.6, 126.1, 125.3, 124.6, 123.5, 122.1, 121.5, 119.6, 117.7. IR (KBr): 3030, 2922, 1618, 1585, 1368, 1358, 1175, 697, 623 cm^{-1}. HRMS (Tesla FTMS): found 463.0518, $C_{28}H_{17}NS_3$ requires 463.0503.

*4.2.3. Synthesis of (E)-4,4′-bis[(2-(dithieno[2,3-b:3′,2′-d]thiophene)-2-yl)vinylphenyl]-N-phenylamine ((E)-**6**).* Dithieno[2,3-*b*:3′,2′-*d*] thiophene-2-carbaldehyde (**4**) (0.33 g, 1.47 mmol) and TPA-$(PPh_3\cdot Br)_2$ (0.64 g, 0.7 mmol, 0.48 equiv) were dissolved in anhydrous tetrahydrofuran (15 mL), solution of potassium *tert*-butoxide (0.38 g, 3.34 mmol, 2.3 equiv) in anhydrous tetrahydrofuran (10 mL) were added dropwise at 0 °C, and then the reaction mixture was warmed slowly up to ambient temperature stir for 6 h. The reaction mixture was quenched with H_2O (10 mL) and extracted with $CHCl_3$ (3×5 mL), then washed with saturated $NaHCO_3$ (2×30 mL) and H_2O (30 mL). The organic layer was dried over anhydrous $MgSO_4$. After the solvent was removed under vacuum, the dry solid was dissolved in 20 mL THF, and then refluxed in presence of catalysis amount iodine for 6 h. Then the mixture was added diluted solution sodium hydroxide to remove iodine, after that extracted it with $CHCl_3$ (3×10 mL). Organic layer was dried with anhydrous sodium sulfate and removed the solvent, and was purified by column chromatography on silica gel with petrol ether, and then petrol ether/$CHCl_3$ (3:1, v/v) as eluent to give (*E*)-**6** (0.21 g, 46%) as a yellow solid. Mp: 252–253 °C. ^{1}H NMR ($CDCl_3$, 400 MHz) δ (ppm): 7.41–7.34 (m, 8H), 7.32–7.28 (m, 4H), 7.19–7.13 (m, 4H), 7.08 (d, J=8.0 Hz, 5H), 6.87 (d, J=16 Hz, 2H), ^{13}C NMR (pyridine-d_5, 100 MHz): δ 148.0, 147.7, 146.9, 140.2, 139.5, 139.3, 138.9, 132.4, 130.4, 129.4, 128.34, 128.3, 125.6, 124.7, 124.4, 122.2, 119.8, 118.7. IR (KBr): 2924, 2853, 1621, 1593, 1360, 1324, 696, 667 cm^{-1}. HRMS (Tesla FTMS): found 685.0149, $C_{38}H_{23}NS_6$ requires 685.0161.

*4.2.4. Synthesis of N-phenyl-N,N-dinaphtho[2,1-b]thieno[2,3-b:3′,2′-d]dithiophene-5-yl-amine (**2**).* To a solution of (*E*)-**6** (30.0 mg, 0.04 mmol) in dry benzene (30 mL), iodine (6.0 mg, 0.02 mmol, 0.5 equiv) was added. The reaction solution was irradiated with a 450 W unfiltered Hg medium pressure lamp. The reaction was monitored by TLC every 20 min, and irradiation was stopped when the (*E*)-**6** was consumed up. After normal workup, the crude product was purified by column chromatography on silica gel with petrol ether (60–90 °C)/$CHCl_3$ (7:1, v/v) as eluent. The collected product was dissolved in $CHCl_3$ and precipitated with MeOH. The precipitate was collected by filtration to afford the target molecule as a pale yellow solid **2** (20 mg, 65%). Mp: 289–290 °C. ^{1}H NMR ($CDCl_3$, 400 MHz) δ (ppm): 8.73 (s, 2H), 7.96 (d, J=8.8 Hz, 2H), 7.81 (d, J=8.8 Hz, 2H), 7.75 (d, J=8.4 Hz, 2H), 7.60 (dd, J=8.8,1.6 Hz, 2H), 7.51–7.44 (m, 4H), 7.31–7.28 (m, 1H), 6.50 (d, J=5.2 Hz, 2H), 6.46 (d, J=5.6 Hz, 2H), ^{13}C NMR ($CDCl_3$, 100 MHz): δ 148.8, 146.9, 141.2, 140.0, 139.3, 138.5, 133.8, 130.2, 128.5, 128.1, 126.1, 125.9, 124.6, 124.0, 123.2, 121.3, 120.2, 119.4. IR (KBr): 2921, 1616, 1384, 1115, 694 cm^{-1}. HRMS (Tesla FTMS): found 680.9836, $C_{38}H_{19}NS_6$ requires 680.9820.

*4.2.5. Synthesis of tris[(E)-4-(2-dithieno[2,3-b: 3′,2′-d]thiophen-2-yl-vinyl)phenyl] amine ((E)-**7**).* Dithieno[2,3-*b*:3′,2′-*d*]thiophene-2-carbaldehyde (**4**) (70 mg 0.29 mmol) and TPA-$(PPh_3\cdot Br)_3$ (0.12 g, 0.09 mmol, 0.3 equiv) were dissolved in anhydrous tetrahydrofuran (10 mL), a solution of potassium *tert*-butoxide (50 mg, 0.41 mmol, 1.4 equiv) in anhydrous tetrahydrofuran (8 mL) were added dropwise at 0 °C, and then the reaction mixture was warmed slowly to ambient temperature stir for 6 h. The reaction mixture was quenched with H_2O (10 mL) and extracted with $CHCl_3$ (3×5 mL), then washed with saturated $NaHCO_3$ (2×20 mL) and H_2O (20 mL). The organic layer was dried over anhydrous $MgSO_4$. After the solvent was removed under vacuum, the collected product was dissolved in $CHCl_3$ and precipitated in MeOH. The precipitate was collected by filtration to afford the target molecule as a pale yellow solid (*E*)-**7** (0.06 g, 68%). Mp: >300 °C. ^{1}H NMR ($CDCl_3$, 400 MHz) δ (ppm): 7.41–7.39 (m, 9H), 7.34 (d, J=5.2 Hz, 3H), 7.30 (s, 3H), 7.19 (d, J=16.0 Hz, 3H), 7.11 (d, J=8.4 Hz, 6H), 6.88 (d, J=16.0 Hz, 3H), ^{13}C NMR (pyridine-d_5, 100 MHz): δ 147.4, 146.9, 140.2, 139.5, 139.4, 139.0, 132.8, 129.4, 128.4, 128.3, 125.1, 122.4, 119.8, 118.7. IR (KBr): 2922, 1595, 1384, 1322, 696, 663 cm^{-1}. HRMS (Tesla FTMS): found 904.9624, $C_{48}H_{27}NS_9$ requires 904.9631.

*4.2.6. Synthesis of N,N,N-tri(naphtho[2,1-b]thieno-[2,3-b:3′,2′-d]dithiophene-5-yl)amine (**3**).* To a solution of (*E*)-**7** (30 mg, 0.03 mmol) in dry benzene (30 mL), iodine (4.2 mg, 0.02 mmol, 0.5 equiv) was added. The reaction solution was irradiated with a 450 W unfiltered Hg medium pressure lamp. The reaction was monitored by TLC every 20 min, and irradiation was stopped when the (*E*)-**7** was consumed up. After normal workup, the crude product was purified by column chromatography on silica gel with petrol ether (60–90 °C)/$CHCl_3$ (3:1, v/v) as eluent. The collected product was dissolved in $CHCl_3$ and precipitated with MeOH. The precipitate was collected by filtration to afford the target molecule as a pale yellow solid **3** (10 mg, 34%). Mp: >300 °C. ^{1}H NMR ($CDCl_3$, 400 MHz) δ (ppm): 8.86 (s, 3H), 8.10 (d, J=8.8 Hz, 3H), 7.93 (d, J=8.8 Hz, 3H), 7.85 (d, J=8.4 Hz, 3H), 7.81 (dd, J=8.0, 2.0 Hz, 3H), 6.20 (d, J=5.2 Hz, 3H), 5.76 (d, J=5.2 Hz, 3H). IR (KBr): 2921, 1611, 1508, 1384, 1360, 1331, 1267, 692, 652 cm^{-1}. HRMS (Tesla FTMS): found 898.9155, $C_{48}H_{21}NS_9$ requires 898.9172.

Acknowledgements

We thank Mr. Pengtao Ma for crystal measurements. This research was supported by National Natural Science Foundation of China (21270255, U1304207, 20972041), Program for SRFDP (20124103110004) and Program of Henan University (SBGJ090506).

Supplementary data

Supplementary data associated with this article can be found in the online version, at http://dx.doi.org/10.1016/j.tet.2014.04.031.

These data include MOL file and InChiKeys of the most important compounds described in this article.

References and notes

1. (a) Shen, Y.; Chen, C.-F. *Chem. Rev.* **2012**, *112*, 1463–1535; (b) Aloui, F.; Moussa, S.; Hassine, B. B. *Tetrahedron Lett.* **2012**, *53*, 3216–3219; (c) Crittall, M. R.; Rzepa, H. S.; Carbery, D. R. *Org. Lett.* **2011**, *13*, 1250–1253; (d) Kelgtermans, H.; Dobrzańska, L.; Meervelt, L. V.; Dehaen, W. *Org. Lett.* **2012**, *14*, 5200–5203.
2. (a) Žádný, J.; Jančařík, A.; Andronova, A.; Šámal, M.; Chocholoušová, J. V.; Vacek, J.; Pohl, R.; Šaman, D.; Císařová, I.; Stará, I. G.; Starý, I. *Angew. Chem., Int. Ed.* **2012**, *51*, 5857–5861; (b) Krausová, Z.; Sehnal, P.; Bondzic, B. P.; Chercheja, S.; Eilbracht, P.; Stará, I. G.; Šaman, D.; Starý, I. *Eur. J. Org. Chem.* **2011**, 3849–3857; (c) Shibata, T.; Uchiyama, T.; Yoshinami, Y.; Takayasu, S.; Tsuchikama, K.; Endo, K. *Chem. Commun.* **2012**, 1311–1313.
3. (a) Grimme, S.; Harren, J.; Sobanski, A.; Vögtle, F. *Eur. J. Org. Chem.* **1998**, 1491–1509; (b) Katz, T. J. *Angew. Chem., Int. Ed.* **2000**, *39*, 1921–1923; (c) Huang, Y.; Fu, L.; Zou, W.; Zhang, F.; Wei, Z. *J. Phys. Chem. C* **2010**, *115*, 10399–10404; (d) Norel, L.; Rudolph, M.; Vanthuyne, N.; Williams, J. A. G.; Lescop, C.; Roussel, C.; Autschbach, J.; Crassous, J.; Réau, R. *Angew. Chem.* **2010**, *122*, 103–106; *Angew. Chem., Int. Ed.* **2010**, *49*, 99–102; (e) Maeda, H.; Bando, Y.; Shimomura, K.; Yamada, I.; Naito, M.; Nobusawa, K.; Tsumatori, H.; Kawai, T. *J. Am. Chem. Soc.* **2011**, *133*, 9266–9269.
4. Talele, H. R.; Sahoo, S.; Bedekar, A. V. *Org. Lett.* **2012**, *14*, 3166–3169.
5. (a) Wynberg, H. *Acc. Chem. Res.* **1971**, *4*, 65–73; (b) Tovar, J. D.; Rose, A.; Swager, T. M. *J. Am. Chem. Soc.* **2002**, *124*, 7762–7769; (c) Moussa, S.; Aloui, F.; Hassine, B. B. *Tetrahedron Lett.* **2012**, *53*, 5824–5827.
6. Dumitrascu, F.; Dumitrescu, D. G.; Aron, I. *Arkivoc* **2010**, 1–32.
7. (a) Waghray, D.; Zhang, J.; Jacobs, J.; Nulens, W.; Basarić, N.; Meervelt, L. V.; Dehaen, W. *J. Org. Chem.* **2012**, *77*, 10176–10183; (b) Bell, J. W.; Hext, N. M. *Chem. Soc. Rev.* **2004**, *33*, 589–598.
8. (a) Wang, Z. H.; Shi, J. W.; Wang, J. G.; Li, C. L.; Tian, X. Y.; Cheng, Y. X.; Wang, H. *Org. Lett.* **2010**, *12*, 456–459; (b) Li, C. L.; Shi, J. W.; Xu, L.; Wang, Y. G.; Cheng, Y. X.; Wang, H. *J. Org. Chem.* **2009**, *74*, 408–411; (c) Liu, X. M.; Yu, P. P.; Xu, L.; Yang, J. J.; Shi, J. W.; Wang, Z. H.; Cheng, Y. X.; Wang, H. *J. Org. Chem.* **2013**, *78*, 6316–6321; (d) Sun, H. L.; Shi, J. W.; Zhang, Z. L.; Zhang, S.; Liang, Z. L.; Wan, S. S.; Cheng, Y. X.; Wang, H. *J. Org. Chem.* **2013**, *78*, 6271–6275.
9. (a) Ripaud, E.; Olivier, Y.; Leriche, P.; Cornil, J.; Roncali, J. *J. Phys. Chem. B* **2011**, *115*, 9379–9386; (b) Fan, C.; Wang, X.; Ding, P.; Wang, J.; Liang, Z.; Tao, X. *Dyes Pigments* **2012**, *95*, 757–767.
10. (a) Zhao, D. F.; Xu, L.; Wang, H. *J. Henan Univ. (Nat. Sci.)* **2007**, *37*, 468–473; (b) Wang, Z.; Zhao, C. M.; Zhao, D. F.; Li, C. L.; Zhang, J. L.; Wang, H. *Tetrahedron* **2010**, *66*, 2168–2174.
11. Tian, H.; Yang, X.; Chen, R.; Zhang, R.; Hagfeldt, A.; Sun, L. *J. Phys. Chem. C* **2008**, *112*, 11023–11033.
12. Sobolev, A. N.; Belsky, V. K.; Romm, I. P.; Chernikova, N. Y.; Guryanova, E. N. *Acta Crystallogr.* **1985**, *C41*, 967–971.
13. Frisch, G. W. T. M. J.; Schlegel, H. B.; Scuseria, G. E.; Robb, M. A.; Cheeseman, J. R.; Montgomery, J. A.; Vreven, T., Jr.; Kudin, K. N.; Burant, J. C.; Millam, J. M.; Iyengar, S. S.; Tomasi, J.; Barone, V.; Mennucci, B.; Cossi, M.; Scalmani, G.; Rega, N.; Petersson, G. A.; Nakatsuji, H.; Hada, M.; Ehara, M.; Toyota, K.; Fukuda, R.; Hasegawa, J.; Ishida, M.; Nakajima, T.; Honda, Y.; Kitao, O.; Nakai, H.; Klene, M.; Li, X.; Knox, J. E.; Hratchian, H. P.; Cross, J. B.; Adamo, C.; Jaramillo, J.; Gomperts, R.; Stratmann, R. E.; Yazyev, O.; Austin, A. J.; Cammi, R.; Pomelli, C.; Ochterski, J. W.; Ayala, P. Y.; Morokuma, K.; Voth, G. A.; Salvador, P.; Dannenberg, J. J.; Zakrzewski, V. G.; Dapprich, S.; Daniels, A. D.; Strain, M. C.; Farkas, O.; Malick, D. K.; Rabuck, A. D.; Raghavachari, K.; Foresman, J. B.; Ortiz, J. V.; Cui, Q.; Baboul, A. G.; Clifford, S.; Cioslowski, J.; Stefanov, B. B.; Liu, G.; Liashenko, A.; Piskorz, P.; Komaromi, I.; Martin, R. L.; Fox, D. J.; Keith, T.; Al-Laham, M. A.; Peng, C. Y.; Nanayakkara, A.; Challacombe, M.; Gill, P. M. W.; Johnson, B.; Chen, W.; Wong, M. W.; Gonzalez, C.; Pople, J. A. *Gaussian 03W, Revision C.02*; Gaussian: Wallingford, CT, 2004.